Book of Tutorials and Abstracts

European Microbeam Analysis Society

EMAS 2025

18th

EUROPEAN WORKSHOP

on

MODERN DEVELOPMENTS AND APPLICATIONS IN MICROBEAM ANALYSIS

11 to 15 May 2025
at the
TecnoCampus
Mataró (Barcelona), Spain

Organized in collaboration with the
Universitat de Barcelona, Spain

EMAS
European Microbeam Analysis Society eV
www.microbeamanalysis.eu/

This volume is published by:
European Microbeam Analysis Society eV (EMAS)
EMAS Secretariat
c/o Eidgenössische Technische Hochschule, Institut für Geochemie und Petrologie
Clausiusstrasse 25
8092 Zürich
Switzerland

ISBN 978 90 8227 6985
NUR code: 972 – Materials Science

QUANTITATIVE MAPPING OF NITROGEN IN Ti-6Al-4V: DEVELOPMENT AND APPLICATION OF A NOVEL COMBINED SXES, EDS AND WDS TECHNIQUE

Jon W. Fellowes[1], D. Hu[2], R. Biswal[3,4], S. Williams[3] and A.E. Davis[2]

1 University of Manchester, Faculty of Science of Engineering, Electron Microscopy Centre
Oxford Road, Manchester M13 9PL, Greta Britain
2 University of Manchester, Department of Materials
Manchester M13 9PL, Greta Britain
3 Cranfield University, Welding Engineering and Additive Manufacturing Centre
College Road, Cranfield MK43 0PL, Great Britain
4 Now at Digital Engineering Group, Manufacturing Technology Centre
Coventry CV7 9JU, Great Britain
e-mail: jonathan.fellowes@manchester.ac.uk

Jon Fellowes is a senior experimental officer at the University of Manchester with over 10 years' experience with electron microprobes. Jon splits his time between microanalysis studies in the Department of Earth Sciences using a CAMECA SX100 to investigate a wide range of Earth and planetary specimens, and the Department of Materials where he is responsible for the operation of a JEOL 8530F FEG-EPMA. Jon has a particular research interest in the quantitative analysis of light elements using the UK's first soft X-ray emission spectrometer (SXES-LR), and is a co-investigator on the UK-wide "Quantitative electron-beam X-ray microanalysis (SEM and EPMA) in Earth and Environmental Science" training course.

1. ABSTRACT

The nitrogen content of Ti-alloys can be used to constrain the metallurgical characteristics of additively manufactured (AM) products, however, spatial and quantitative determination is hindered by a number of analytical challenges. This work describes the development and application of a novel combined EDS, WDS and SXES methodology for the simultaneous sub-micrometre and macro scale quantification of nitrogen in an AM Ti-6Al-4V specimen.

2. INTRODUCTION

Additive manufacturing (AM) methods, and in particular wire-arc additive manufacturing (WAAM), are ideal for the fabrication of large-scale parts in the aerospace industry, with high deposition rates in the 'kg/h' range, high material utilisation and the ability to manufacture near net-shape components [1, 2]. The α-β titanium alloy Ti-6Al-4V (Ti64) sees substantial use in the aerospace industry due to a range of desirable metallurgical characteristics including corrosion resistance, high specific strength, and fracture resistance [3]. Traditional machining of Ti64 produces significant levels of Ti64 swarf, and recycling and reuse of this waste product in novel AM processes can reduce energy consumption and CO_2 emissions [4]. The use of recycled waste products as AM feedstock material can introduce contaminants such as C, N, O and Fe into the built products, leading to adverse effects on the product performance. Nitrogen in particular is an α-stabiliser and is known to have a similar role as oxygen in increasing the β-transus temperature (T_β) [5], with important implications in AM using Ti64 as thermal cycling below T_β causes a partial α-β phase transformation producing heat affected zone (HAZ) bands [6]. This issue is compounded by the heterogeneous distribution of N in AM-built products using Ti64 waste products with a variable N content. It is, therefore, highly desirable to be able to determine the concentration and spatial distribution of N in Ti64. Traditional metallographic assaying techniques face major hurdles in the application to N quantification in Ti64, whether lacking sufficiently high spatial resolution to determine the N-distribution within a component on a sub-micrometre scale (e.g., inductively couple plasma, ICP); requiring prohibitive amounts of analytical time to determine the N-content on the millimetre scale (e.g., atom probe tomography, APT); lack the ability to accurately produce quantitative results (e.g., secondary ion mass spectrometry, SIMS), or lack the spectral resolution or sensitivity required to separate the N from other X-ray emissions (e.g., scanning electron microscopy – energy-dispersive X-ray spectrometry (SEM-EDS), transmission electron microscopy - EDS (TEM-EDS), electron probe microanalyser – wavelength-dispersive X-ray spectrometry (EPMA/WDS)) [7].

This work will detail the development of a novel methodology using combined, simultaneous EDS, WDS and soft X-ray emission spectroscopy (SXES) to spatially resolve and quantify the N-concentration in the macro and microstructure of a WAAM Ti64 specimen built initially under an inert Ar and subsequently an N_2 enriched atmosphere.

3. MATERIALS AND METHODS

A Ti64 WAAM wall specimen with varied N-concentration was built by first depositing 15 layers using a N-lean (~ 0.007 wt% N) Ti64 wire spool under an inert Ar atmosphere followed by 20 layers under an N_2/Ar gas mix with a volumetric ratio of 0.11. The inert Ar atmosphere was maintained until the temperature of the solidified melt pool dropped below 500 °C. Below this temperature the ingress of N into Ti64 is negligible. Full details of the Ti64 WAAM wall specimen build can be found elsewhere [4]. The sample was ground and polished using standard metallographic electron microscopy preparation techniques and the sample was plasma cleaned in an Ar/O_2 plasma immediately prior to loading for analysis.

The sample was analysed at the University of Manchester using a JEOL JXA-8530F FEG-EPMA equipped with 4 WDS each equipped with a number of diffraction crystals, a JEOL EX-94310F4L1Q SDD EDS detector with a 10 mm^2 effective detection area and 129 eV spectral resolution, and a JEOL SS-94000 SXES equipped with the JS200N varied line spacing (VLS) diffraction grating and a 2048 × 2048 pixel non-coated, back-illuminated CCD [8]. All EDS and WDS specimen map data was collected using the JEOL PC-EPMA software. EDS and WDS standards were acquired using the Probe Software Inc. PROBE FOR EPMA software. SXES standards and specimen maps were acquired simultaneously using the CSIRO NiCoLiN software. In-house developed software was used to reduce the EDS and SXES data into the correct format for input into the PROBE FOR EPMA and CALCIMAGE software for standardisation and map quantification, respectively. The instrument was operated with a 10 kV accelerating voltage, a beam current of 115 nA, a beam diameter of approximately 100 nm and a map dwell time of 5,000 ms per pixel. The accelerating voltage chosen was a compromise: High enough to ensure sufficient emission intensity of the Fe-Kα as well as low enough for sufficient emission intensity of the N-Kα. Monte Carlo simulation of a N- and Fe-enriched Ti64 phase at 10 kV accelerating voltage using the CASINO software indicates an emission depth for all measured elements of < 500 nm and an emission radius of approximately 250 nm from the beam centre for the majority of X-ray emissions. The dwell time chosen was to ensure sufficient counts were obtained to differentiate the N-Kα II from the Ti-Ll II. Two maps were taken of the Ti64 specimen: (*i*) a "low mag" stage scan map with a step size of 40 μm covering an area of approximately 8 mm^2 to show macro-scale N-variability between the inert and N_2-enriched WAAM atmosphere, and (*ii*) a "high mag" stage scan map with a step size of 500 nm and an area of 50 μm^2 to show segregation of N between the α- and β-phases in the N-enriched area of the WAAM Ti64 sample. Total analysis time was ~ 62 hours for the "low mag" analysis and ~ 14 hours for the "high mag" analysis.

3.1. WDS quantification of Al, V and Fe

Al-Kα, V-Kα and Fe-Kα were measured on TAP, LIFL and LIFL diffraction crystals, respectively. The TAP spectrometer is equipped with a P_{10} gas flow proportional counter, the LIFL spectrometers are equipped with sealed Xe-filled proportional counters. V-Kα had

an interference correction applied for Ti-Kβ interference. Al, V and Fe was quantified relative to pure metal standards. Background correction was via the mean atomic number (MAN) background method [9].

3.2. EDS Quantification of Ti

EDS spectra were collected using the JEOL EDS via the integrated PROBE FOR EPMA interface for a range of standard materials including the primary standards used for quantification of Ti, Al, V, Fe and N. Ti was measured by EDS with a summed area between approximately 4.30 and 4.72 keV incorporating the Ti-K$\alpha_{1,2}$ emission peaks. This integrated emission intensity was then reinserted in the PROBE FOR EPMA MDB database file for use to create a Ti-Kα by EDS MAN background curve. No equivalent EDS software integration exists to obtain Ti-K$\alpha_{1,2}$ emission net intensity maps from EDS hypercubes collected during Ti64 specimen map acquisition using the JEOL PC-EPMA software, and so bespoke software was created to extract the raw EDS hypercube from the acquired data. This extracted and integrated raw emission intensity was then deadtime and pulse pileup corrected before being converted to the Golden Software GRD format for use in CALCIMAGE.

3.3. SXES Quantification of N

2nd order N-Kα was measured using the JS200N diffraction grating of the SXES and quantified relative to a TiN standard. Owing to the significant overlap of the N-Kα II and the 2nd order Ti-Ll (Ti $L_{2,3}$-M) emissions and the complex background shape arising from Ti plasmon satellite and Ti-Lη II emissions (Fig. 1), the whole region between approximately 168 eV and 206 eV was extracted from the SXES hypercube for the Ti64 sample, and the Ti metal and TiN standards. An exponential background was fitted based on averaging the intensity of the five channels around 168 eV and 206 eV and subtracted from the above spectra. To deconvolve the N-Kα II from the Ti-Ll II and other Ti-emissions, the background-subtracted Ti metal spectrum was scaled to the emission intensity of Ti Ll II emission for each TiN standard spectra and per pixel spectra (e.g., X, Y) of the Ti64 map and subtracted (see Fig. 1). The background-subtracted and deconvolved N-Kα II emission was then summed between approximately 194 eV and 197 eV to avoid the variable effect of the Ti-Lη II emission [10]. For the TiN standard, the deconvolved N-Kα II summed emission intensity was entered into a modified PROBE FOR EPMA MDB database file for use as the TiN standard intensity already corrected for deadtime, background and on-peak interference. For the Ti64 map, Golden Software GRD-format files were created for quantification within the CALCIMAGE software.

Once the WDS, EDS and SXES contributions were combined into single quantification analyses for the “low mag” and “high mag” samples respectively, the maps were fully quantified in CALCIMAGE for background, interference, matrix and standard drift effects. The PAP PRZ matrix correction routine was used along with the NIST FFAST MAC tables.

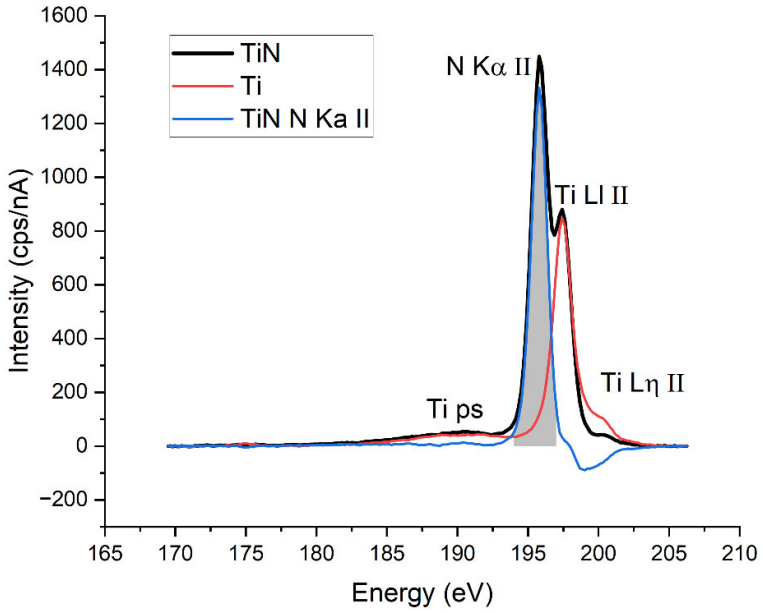

Figure 1. Extracted background subtracted N-Kα II region for the average TiN standard (black line), the Ti metal standard (red line) and the Ti-interference corrected N-Kα II from TiN (blue line). The shaded area indicates the summed region for N-Kα II emission intensity. The emission lines for N-Kα II, Ti-Ll II, Ti-Lη II and Ti-plasmon satellites (ps) are labelled.

4. RESULTS AND DISCUSSION

4.1. Quantification of N by SXES

SXES spectra from the N-lean and N-enriched WAAM Ti64 specimen are shown in Fig. 2. The significant overlap between the Ti-Ll II emission and the N-Kα II emission is further complicated by the comparative emission intensities of Ti and N in this sample, with Ti comprising the vast majority of the sample in both N-lean and N-enriched phases meaning the N-Kα II was only visible as a slight shoulder in the N-enriched sample (Fig. 2 main panel). The 2nd order N-Kα emission is the highest order N-Kα emission visible to the SXES-LR with the JS200N grating as used in this study. Although the spectral resolution increases as a function of diffraction order (see Fig. 2 inset), the count rate decreases by approximately a factor of four as order increases and so the 2nd order was chosen for quantification.

Figure 3 shows single pixel (5,000 ms dwell) SXES spectra obtained from the N-rich and N-lean regions of the sample compared with the N-Kα II emission extracted from TiN. The contributions of the Ti plasmon satellites (Ti ps) have been almost completely removed from the resulting deconvolved spectra, along with minimal contributions from the Ti-Ll II and Ti-Lη II emissions. The complete removal of the Ti-Ll II and Ti-Lη II contribution to the entire spectral region studied is unlikely owing to the origin of the Ti-L emissions in this region.

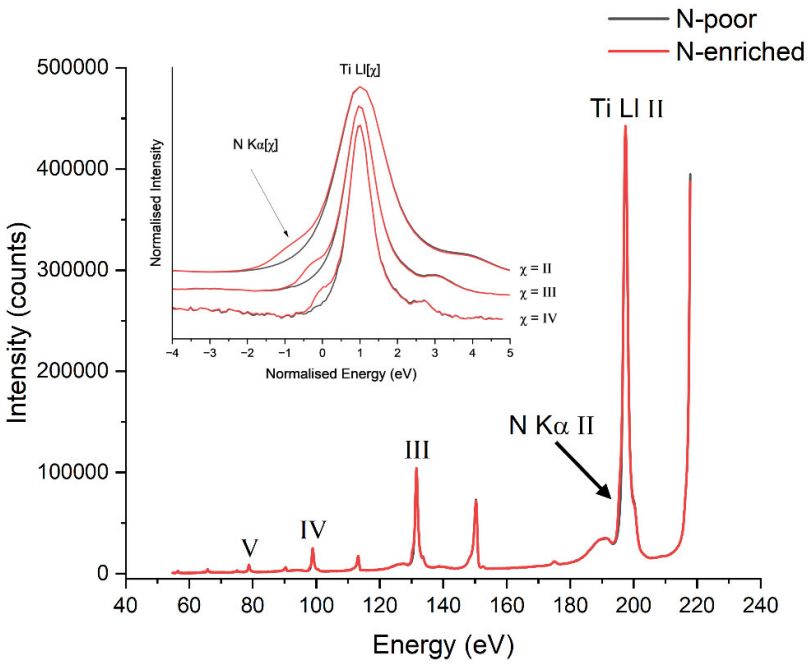

Figure 2. SXES spectra for the N-lean and N-enriched regions of the Ti64 specimen. The relative intensity of the higher order reflections of the Ti-Ll emission are shown, as is the position of the N-Kα II. Inset: The increase in spectral resolution as diffraction order increases (normalised intensity).

The exact energy and shape of the Ti-Ll and Ti-Lη emissions arises from inner-shell electron transitions influenced by the screening of a 3s core-hole [10]. As the exact energy of peak emission intensity and peak shape of the Ti-Ll and Ti-Lη emissions is unique to TiN, it is, therefore, not possible to completely remove the effect of Ti-L emissions on the N-Kα as this would require a TiN phase with no N. As the peak emission intensity of the Ti-Ll II appears to be the same as that for Ti metal, it was decided to use the Ti metal standard (once scaled to an appropriate peak height) to remove the Ti-Ll II from the N-Kα II in TiN and to ensure that the energy region summed for the N-Kα II did not include the area of the Ti-Lη II (see Fig. 1 and Fig. 3 shaded regions), which differs between TiN and Ti metal (see Fig. 1). The increase in spectral noise around 197 – 198 eV corresponds to the peak of Ti-Ll II intensity in TiN and shows that there is likely some small difference in the Ti-Ll II emission between TiN and Ti metal. Nevertheless, this approach has shown that it is possible to almost completely deconvolve the N-Kα II from the Ti-L II emissions to be used for further N quantification in Ti-rich samples. Unlike with traditional WDS measurements that are only able to measure a single wavelength at a time and either (*i*) require time-intensive WDS scanning over the N-Kα emission and integration of the counts, or (*ii*) an area-peak factor correction to account for changes in the N-Kα emission profile, the hyperspectral nature of SXES allows us to sum all channels within a region for quantification and so accounts for variations in peak position and shape between the standard and specimen, and within the specimen map. The large differences in count rate between the standard and unknown specimen can also be accounted for as SXES has been previously shown to not be significantly affected by deadtime issues [11].

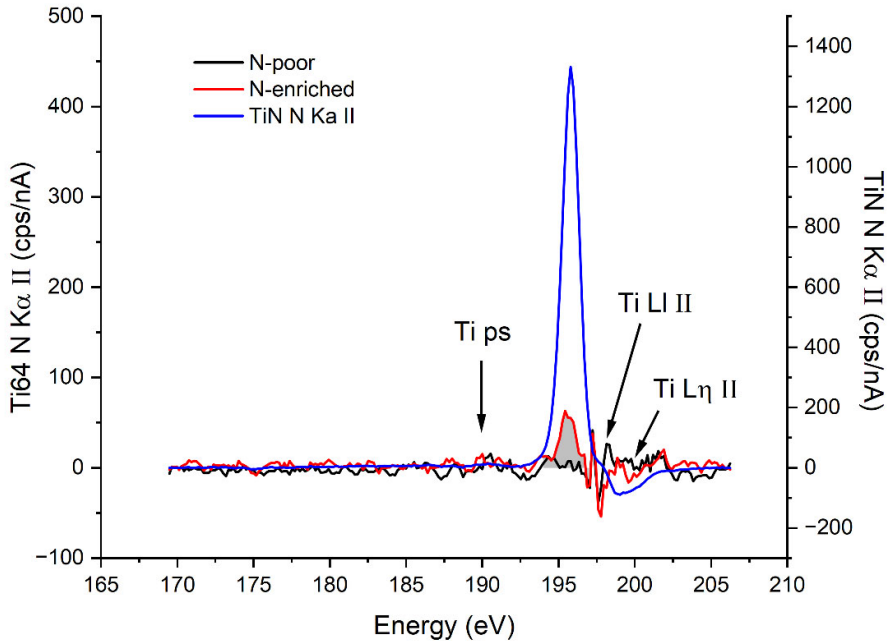

Figure 3. Deconvolved N-Kα II emissions for individual pixels (5,000 ms dwell time) for the N-lean (black) and N-enriched (red) regions of the "low mag" map. Blue line shows the N-Kα II as deconvolved from the TiN standard. The shaded area illustrates the summed energy region used to determine emission intensity.

4.2. Quantification of Ti by EDS

The quantitative determination of major elements such as Ti by EDS in Ti alloys is advantageous as EDS is largely insensitive to drift in the standardisation as seen in WDS with gas flow proportional counters that is largely attributable to variations in barometric pressure and other environmental factors. EDS is also less sensitive to subtle sample height fluctuations that are problematic for Rowland-circle based spectrometers that may occur on the macro-scale as a result of mechanical polishing. Whilst both EDS and WDS detectors are notably affected by deadtime issues [12], the treatment of EDS spectral data to account for this is routine with detector "live times" often included within a dataset. The use of WDS under the conditions required for this study (10 kV accelerating voltage, 115 nA beam current) would create a significant deadtime issue for measuring Ti in this Ti64 specimen using a PET or LiF diffraction element for the first order emission. Two alternative techniques could be employed to use WDS although both have notable drawbacks: (*i*) multiple beam condition analysis that would require significantly decreasing the beam current to drop the Ti count rate in to the "linear" deadtime correction regime for the spectrometer chosen. This would necessitate a second analytical pass over the sample, and the change in beam conditions may lead to an appreciable shift in the beam position between passes; and (*ii*) analysing either a 1st order lower emission intensity line (e.g., Ti-Kβ) or a higher order (and therefore lower intensity) line of the Ti-Kα.

The Ti-Kβ emission in this case would be difficult owing to the significant overlap of the Ti-Kβ with the V-Kα also present as a major element in these samples, and the lower count rate of the higher order lines would produce a greater uncertainty of the Ti concentration, impacting the final analytical total and overall confidence in the measured composition.

Of the alternative detectors available on this instrument to collect quantifiable Ti X-ray emissions, it was decided against using the Ti-L emission lines for quantification using the SXES as above owing to potential self-absorption issues of the Ti-Lα and -Lβ emissions as occurs with e.g., Fe-L [13, 14], the interference between the Ti-Ll and N-Kα, the potential peak shape and energy changes between standard and specimen, and the extra sensitivity of these emissions to any slight oxidation of either the standard or specimen. The JEOL EDS detector as fitted to this EPMA instrument was enabled for all standard and unknown acquisitions, and so it was decided to use this detector for quantification of the Ti-Kα. The OEM software is unable to produce deadtime corrected net intensity maps of EDS spectral regions, and so bespoke software was written that was able to directly open and extract the raw EDS count intensities. It was then possible to extract and correct for the deadtime for both the "low mag" and "high mag" mapped areas (Fig. 4). The mean EDS deadtime for the "high mag" specimen was 34.07 %.

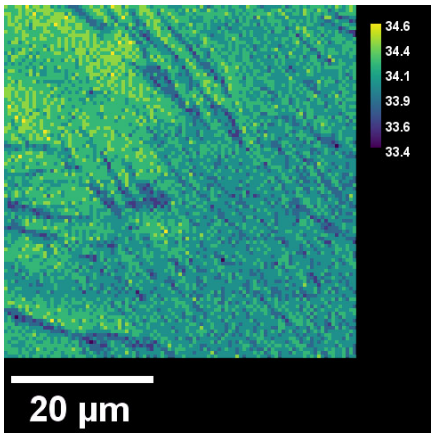

Figure 4. Extracted deadtime for the "high mag" sample. Deadtimes agree with those reported by the OEM JEOL PC-SEM software.

In addition to the deadtime, it was also apparent that pulse pileup correction had not been applied to the raw data extracted from the EDS hypercube, and so an arithmetic correction factor was determined for the pulse pile up (Fig. 5). Application of this correction factor to deadtime-corrected EDS measurements taken of metal standards over a range of beam currents shows agreement to > 99.5 %, suggesting that despite the deviation from the polynomial line of best fit seen in figure 5 (R^2 value of 0.9853), this simple correction is sufficient for precision within 1 %. Investigations on the cause of this variation will be the focus of future work.

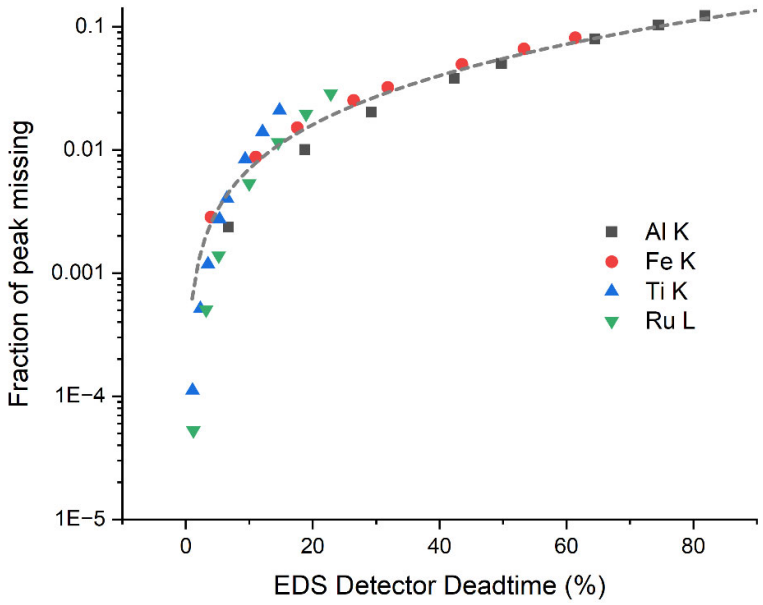

Figure 5. Fraction of the deadtime and background corrected summed energy regions for the Al-Kα, Ti-Kα, Fe-Kα and Ru-Lα emissions expressed as a proportion of the peak thought to be 'missing' due to pulse pile up (as calculated by regression of individual energy region intensities to an EDS detector deadtime of 0 %).

Another factor to consider in the application of simultaneous quantitative EDS is whether the EDS spectra returned to PROBE FOR EPMA by the JEOL EDS API is the same as the data obtained by extracting the raw EDS intensities from the acquired hypercube. To test this, EDS maps were taken of the Ti standard and pixel values were extracted and directly compared to the EDS spectra stored within the PROBE FOR EPMA MDB database (Fig. 6). These results show a strong correlation between the JEOL API and shorter dwell time (20 s versus 5 s) single pixel hypercube spectra with an R^2 value of 0.995 and a line equation of $y = 1.0018x$, suggesting that direct comparison between the standards and specimen is possible. Once deadtime and pulse pileup corrected, it is then necessary to background correct and sum the EDS channels for the desired energy range, in this case between 4.30 and 4.72 keV. Several options for background subtraction of whole EDS spectra are possible, each with various advantages and disadvantages. Any potential background subtraction method needs to be robust enough to deal with short collection time data acquired during the map e.g., 5,000 ms real time less 34 % to give a live time of 3,300 ms, with circa 300k counts acquired per pixel inclusive of both characteristic and Bremsstrahlung X-ray emissions. Background subtraction methods include: (*i*) fitting a linear or exponential curve, which is computationally simple but highly dependent on the noise level of the background points chosen, assuming interference-free background positions can be found; (*ii*) top-hat filtering, a routine spectral transformation technique that can effectively suppress the slowly changing background at the expense of significantly altering the spectral profile. It is not possible to reverse this filtering and so extraction of partial spectra for use alongside WDS and SXES make this method less desirable; and (*iii*) full spectrum simulation and peak fitting, such

as used by the NIST DTSA-II software, is the gold standard of EDS quantification, however is computationally complex, requires in-depth knowledge of a specific EDS detector, and would need to be applied to the > 160,000 noisy EDS spectra without fault. For this work, it was decided to apply the MAN correction of Donovan *et al.* [9] to the acquired EDS data, and to reinsert this information into the PROBE FOR EPMA MDB database file to create a deadtime- and absorption-corrected MAN curve for use with both the standard and specimen EDS measurements. Figure 7 shows the obtained MAN curve and shows a strong correlation between the measured EDS intensity and the mean atomic number of the standard used. This technique is a promising development in the use of the EDS alongside WDS and SXES.

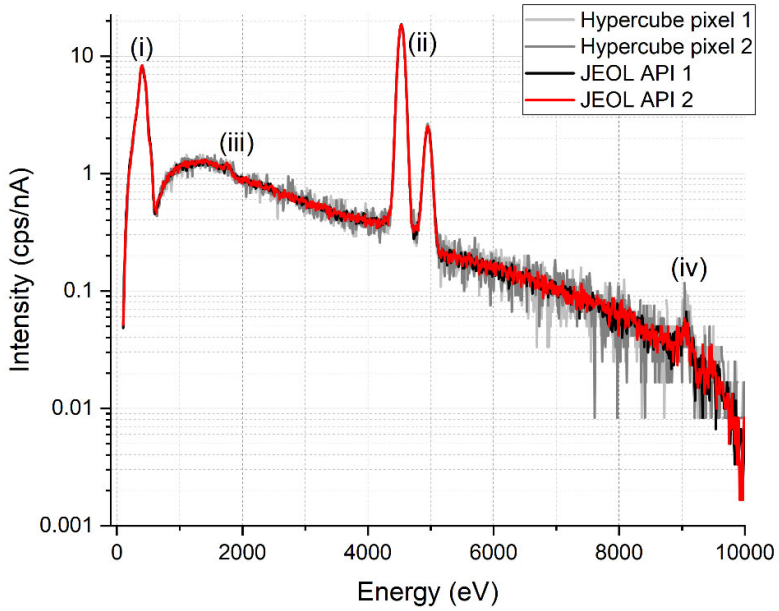

Figure 6. Comparison of the EDS spectra returned to PROBE FOR EPMA by the JEOL EDS API and two individual pixel measurements extracted directly from the EDS map hypercube using software developed for this study. The decrease in noise for the JEOL EDS API returned spectra is due to the longer dwell time per measurement (20 s versus 5 s). Points (i) and (ii) are the Ti-L and Ti-K emissions, respectively. (iii) indicates spectral artefacts arising from the detector (Si-K absorption and Si-Kα emission), (iv) highlights the presence of the Ti-K pile-up peaks.

4.3. Quantitative maps of the "low mag" and "high mag" samples

Figures 8 and 9 show the obtained quantitative maps for Ti (EDS), N (SXES), Al, V and Fe (WDS) for the "low mag" and "high mag" samples. Detailed interpretation of the features arising from this data is discussed elsewhere [4], however these results highlight that the application of the simultaneous combined EDS, SXES and WDS is a valuable tool in the analysis of light elements in Ti -alloys.

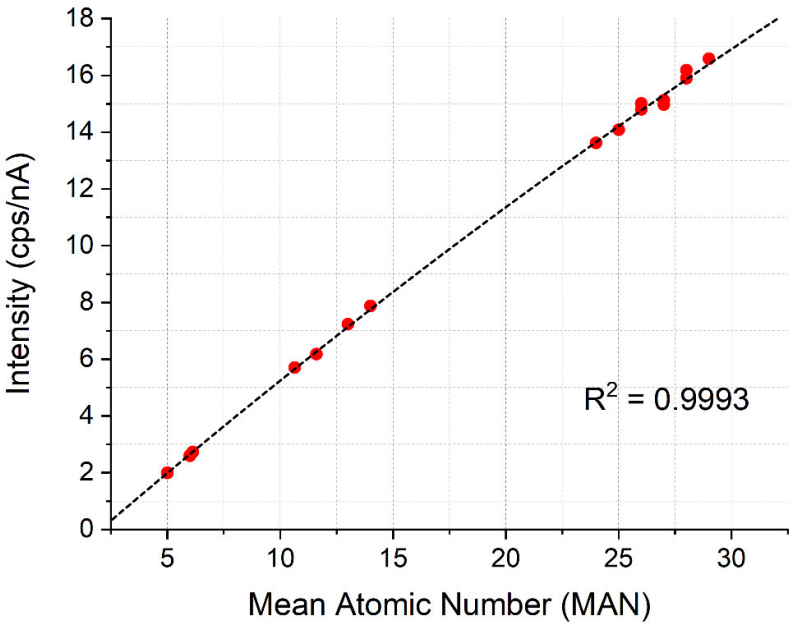

Figure 7. Absorption-corrected MAN background curve for the Ti-Kα energy region extracted, processed and reinserted into the PROBE FOR EPMA MDB database for use in background correction.

The "low mag" SXES N Kα II map (Fig. 8) shows the step change between the initial 15 WAAM layers deposited under an inert atmosphere and the later layers deposited in an Ar:N2 gas mix. A 10 pixel-average line profile (with pixels averaged perpendicular to the line profile direction) taken from the lower N-lean region into the N-enriched region (Fig. 10) in conjunction with measurements extracted by CALCIMAGE shows a N-lean region concentration of ~ 0.017 wt% (0.004 wt% standard error), rising to greater than 1.2 wt% (0.3 wt% standard error). The accuracy of these results compare favourably with ICP measurements of the same sample performed by Hu *et al.* [4], who reported a N-concentration of 0.013 wt% in the "clean" (i.e., N-lean) section of the WAAM build. The discrepancy between the higher concentrations could be caused by variability in the N-content of the N-enriched region or that the nitrogen ICP measurements were outside the range of the instrument calibration. Filtering the "low mag" map analytical totals shows that 41,682 pixels (> 99.98 %) fit between 90 and 105 wt%, with a whole map total of 100.096 wt% (0.7 wt% 1 sigma standard deviation).

The "high mag" map (Fig. 9) shows that this technique can be successfully applied down to spatial resolutions approaching those expected for the analytical volume. The sub-micrometre β-phases can easily be resolved, both by the increase in Fe and V concentrations on the WDS maps and the decrease in Ti and N in the EDS and SXES maps. The EDS, WDS and SXES also show zonation within the α-phase with a relatively Al-poor (WDS) and Ti- (EDS) and N- (SXES) rich region visible on the top left of the map, showing all detectors are in agreement. The slightly

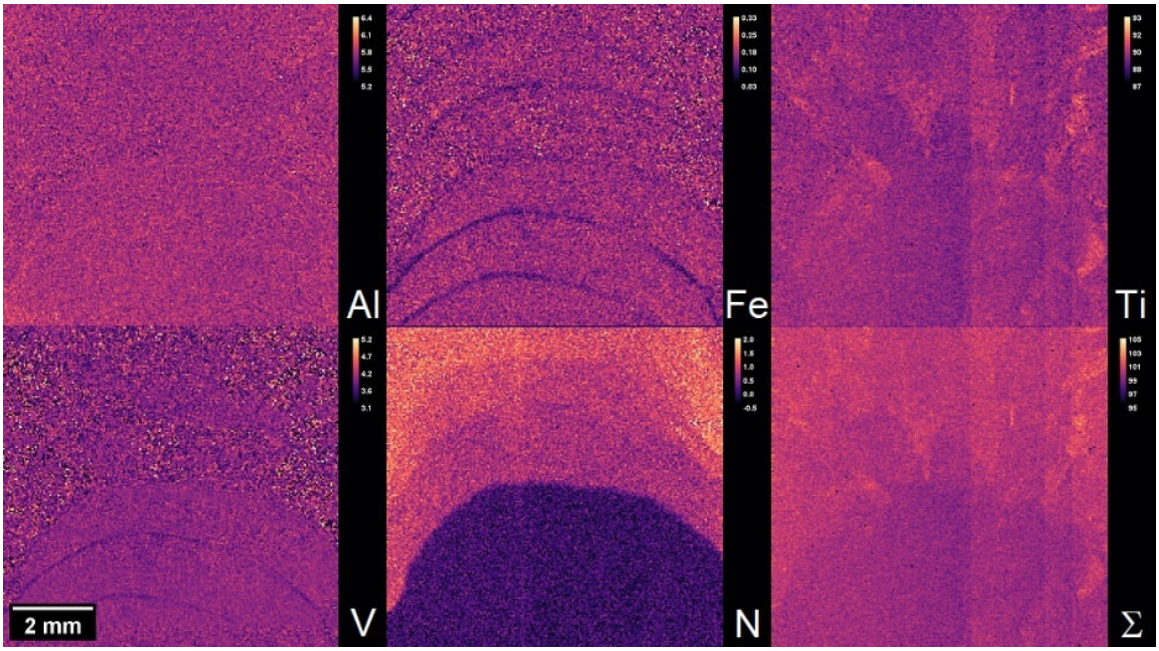

Figure 8. "low mag" quantitative maps obtained by simultaneous SXES, EDS and WDS analysis. Total field of view ~ 8 mm^2. Values on calibration bars are in wt%, Σ is the analytical total.

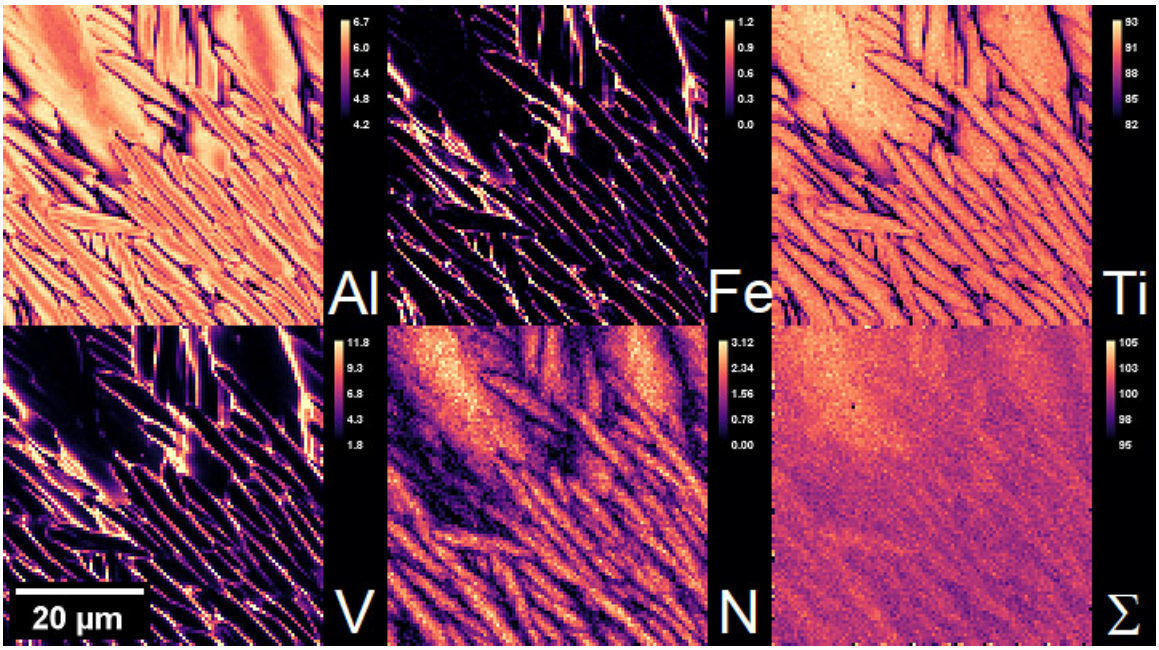

Figure 9. "High mag" quantitative maps obtained by simultaneous SXES, EDS and WDS analysis. Total field of view ~ 50 µm^2. Values on calibration bars are in wt%, Σ is the analytical total.

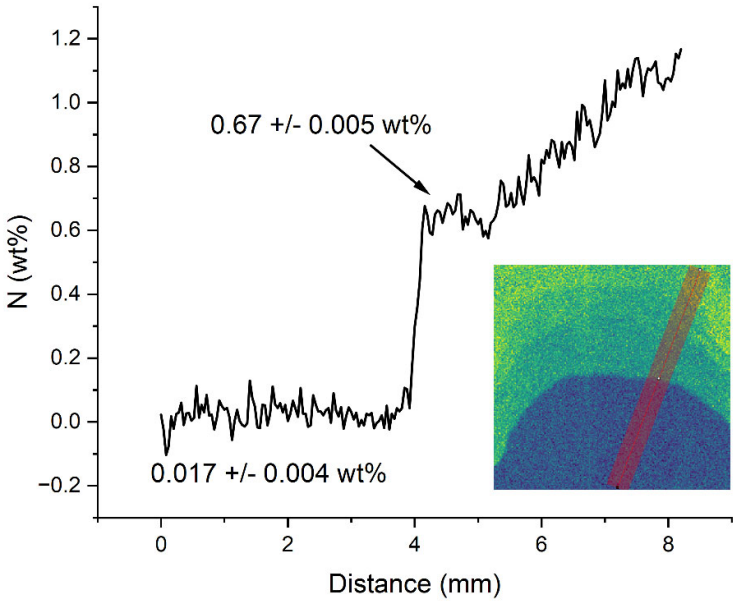

Figure 10. 10 pixel average nitrogen wt% line profile from the N-lean (bottom) to N-enriched (top) of the "low mag" map displayed in Fig. 8. Displayed concentrations are extracted from the individual regions via CALCIMAGE. Errors displayed are 1 standard error. Inset: the selected line profile region.

rich region visible on the top left of the map, showing all detectors are in agreement. The slightly elevated analytical totals (~102 wt%, > 92 wt% Ti) in the top left of the map are thought to derive from a slight oxidation of the pure Ti metal standard.

5. CONCLUSION

This work has developed the simultaneous, quantitative mapping using JEOL EDS, WDS and SXES equipment and applied this to the determination of low concentrations of N within a Ti-rich matrix. The deconvolution of this severe N-Ti interference necessitates the use of the high spectral resolution SXES with an extended dwell time of 5 seconds per pixel. The use of the comparatively stable EDS detector for the determination of major elements over the course of long analyses has been shown to be advantageous, allowing the high sensitivity WDS detectors to be used solely on lower concentration elements and those with severe spectral interferences. This combined methodology will now be used to explore light element relationships in a range of metallic matrices.

6. ACKNOWLEDGEMENTS

The authors are appreciative of the EPSRC programme grant Sustainable Additive Manufacturing (EP/W01906X/1) for supporting this research. This work was supported by the Henry Royce Institute for Advanced Materials, funded through EPSRC grants EP/R00661X/1, EP/S019367/1, EP/P025021/1 and EP/P025498/1.

7. REFERENCES

[1] Gong G, Ye J, Chi Y, Zhao Z, Wang Z, Xia G, Du X, Tian H, Yu H and Chen C 2021 *J. Mater. Res. Technol.* **15** 855-884
[2] Williams S W, Martina F, Addison A C, Ding J, Pardal G and Colegrove P 2016 *Mater. Sci. Tech. Ser*. **32** 641-647
[3] Ezugwu E and Wang Z 1997 *J. Mater. Process. Technol.* **68** 262-274
[4] Hu D, Biswal R, Sahu V K, Fellowes J W, Zadehkabir A, Williams S W and Davis A E 2024 *IOP Conf. Ser.: Mater. Sci. Eng.* **1310** 012020
[5] Welsch G, Boyer R and Collings E 1993 *Materials properties handbook: titanium alloys*. [Materials Park, OH: ASM international]
[6] Ho A, Zhao H, Fellowes J W, Martina F, Davis A E and Prangnell P 2019 *Acta Materialia* **166** 306-323
[7] Gardner H M, Gopon P, Magazzeni C M, Radecka A, Fox K, Rugg D, Wade J, Armstrong D E J, Moody M P and Bagot P A J 2021 *J. Mat. Res.* **36** 2529-2544
[8] Takahashi H, Murano T, Takakura M, Asahina S, Terauchi M, Koike M, Imazono T, Koeda M and Nagano T 2016 *IOP Conf. Ser.: Mater. Sci. Eng.* **109** 012017
[9] Donovan J J and Tingle T N 1996 *Microsc. Microanal.* **2** 1-7
[10] Terauchi M, Koshiya S and Kimito K 2018 *IOP Conf. Ser.: Mater. Sci. Eng.* **304** 012018
[11] Wilson N, MacRae C and Torpy A 2021 *Microsc. Microanal.* **27** (Suppl. 1) 1368-1369
[12] Donovan J J, Moy A, von der Handt A, Gainsforth Z, Maner J L, Nachlas W and Fournelle J 2023 *Microsc. Microanal.* **29** 1096-1110
[13] Buse B and Kearns S 2018 *Microsc. Microanal.* **24** 1-7
[14] Llovet X, Moy A and Fournelle J H 2022 *Microsc. Microanal.* **28** 123-137